J|A|C|S
COMMUNICATIONS

Published on Web 03/20/2007

# Zinc Stannate ($Zn_2SnO_4$) Dye-Sensitized Solar Cells

Bing Tan, Elizabeth Toman, Yanguang Li, and Yiying Wu*

*Department of Chemistry, The Ohio State University, Columbus, Ohio 43210*

Received February 4, 2007; E-mail: wu@chemistry.ohio-state.edu

Dye-sensitized solar cells (DSSCs) have attracted extensive attention due to their low fabrication cost and relatively high efficiency. In a DSSC, a porous electrode made of a wide-band gap semiconductor with long electron diffusion length is needed for supporting dye molecules and transporting photoinjected electrons. Previous research has been limited to simple binary oxides, including $TiO_2$,[1] ZnO,[2] $SnO_2$,[3] $Nb_2O_5$,[4] and $In_2O_3$.[5] In contrast, the application of multication oxides has been rarely explored. To our best knowledge, the only reported ternary oxides are $SrTiO_3$[6] and some doped binary oxides such as $La^{3+}$- and $Zr^{4+}$-doped $CeO_2$.[7]

In comparison with simple binary oxides, multication oxides have more freedom to tune the materials' chemical and physical properties by altering the compositions. As an example, $ZnO-In_2O_3$ ternary compounds have been investigated as new n-type transparent conducting oxide (TCO) materials.[8] By varying the relative Zn/In ratio, the band gap energy, the work function, and the electric resistivity of the ternary oxides can be readily tuned. The ternary oxides also show dramatically reduced acid etching rate in comparison with ZnO. Considering the availability of a wide range of multication oxides and their tunable properties, it is, therefore, interesting to investigate their applications in DSSC. Potentially, new materials with better performance than anatase $TiO_2$ could be found. This strategy is similar to the search of new TCO materials, which, historically, also started with simple binary oxide materials and then have been gradually expanded to many multicomponent oxides.[8]

In this communication, we report the promising application of $Zn_2SnO_4$ nanoparticles in DSSC. $Zn_2SnO_4$ is a TCO material with a band gap of 3.6 eV and electron mobility of 10−15 $cm^2\ V^{-1}\ s^{-1}$.[9] For the application in DSSC, it is desirable to control the particle size in the range of tens of nanometers to ensure high surface area for dye adsorption. The controlled synthesis of $Zn_2SnO_4$ nanoparticles is achieved by decomposing a mixture of zinc and tin *tert*-butylamine complexes under hydrothermal conditions. In a typical synthesis, 0.525 g of zinc chloride (98%, Aldrich) and 0.675 g of tin(IV) chloride pentahydrate (98%, Aldrich) were stirred in 50 mL of water/ethylene glycol (1:1 volume ratio) mixed solvent. Then 25 mL of 1.3 M *tert*-butylamine (99%, Acros Organics) aqueous solution was added dropwise to the stirred solution. After stirring for several minutes, the obtained slurry was transferred to a 125 mL autoclave (Parr Instrument) and heated statically at 175 °C overnight. The precipitates from the autoclave were washed several times with water to remove the left amine.

The obtained product was characterized with X-ray diffraction (XRD, Rigaku) and transmission electron microscopy (TEM, Tecnai TF-20). XRD pattern (Figure 1a) confirms that the product is pure $Zn_2SnO_4$ with the cubic inverse-spinel crystal structure. The average crystal size calculated is around 20 nm. Low-magnification TEM (Figure 1b) shows that most obtained nanoparticles have a size in the range of 10−60 nm. This is desirable to provide high surface area for DSSC application. The crystallinity of nanoparticles was further confirmed by the selected-area electron diffraction pattern (Figure 1c) and high-resolution TEM (Figure 1d).

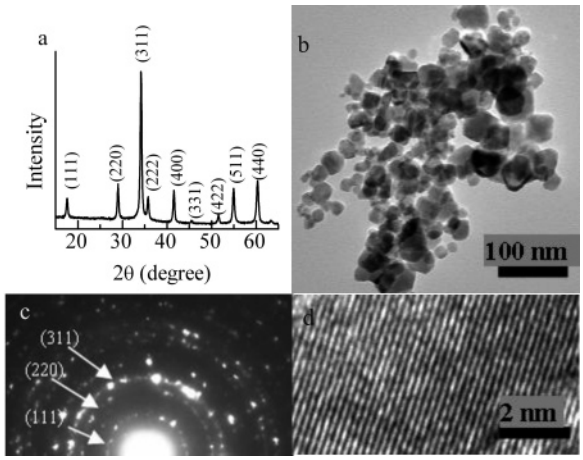


***Figure 1.*** Characterizations of zinc stannate nanoparticles: (a) XRD pattern; (b) low-magnification TEM image; (c) electron diffraction pattern; and (d) high-resolution TEM image (distance between adjacent planes is 2.6 Å, corresponding to *d*-spacing of (311) planes).

***Table 1.*** Dye Adsorption and the *I*−*V* Characteristics (under 1 sun AM 1.5 illumination) for Cells Sensitized with Various Times

| time | roughness factor | $J_{sc}$ ($mA/cm^2$) | $V_{oc}$ (V) | fill factor | efficiency (%) |
|---|---|---|---|---|---|
| 2 h | 209 | 7.6 | 0.63 | 0.65 | 3.1 |
| 6 h | 275 | 8.1 | 0.63 | 0.63 | 3.2 |
| 1 day | 315 | 9.1 | 0.63 | 0.65 | 3.7 |
| 3 days | 338 | 8.8 | 0.63 | 0.64 | 3.6 |
| 7 days | 304 | 9.0 | 0.63 | 0.65 | 3.7 |

The stability of $Zn_2SnO_4$ nanoparticles in an acidic dye solution is examined. The solar cell dye used in this investigation is *cis*-bis(isothiocyanato)bis(2,2′-bipyridyl-4,4′-dicarboxylato)ruthenium(II) bis-tetrabutylammonium (also referred to as N719 or [$RuL_2(NCS)_2$]). Five $Zn_2SnO_4$ DSSCs with the same thickness (~4.3 $\mu$m) were prepared with different sensitization times (Table 1). The dye adsorption (expressed as roughness factor, which is defined as the total surface area per unit substrate area) first increases quickly with the sensitization time in the initial 2 or 6 h and then becomes saturated after 1 day. Under 1 sun AM 1.5 illumination, the short-circuit current density ($J_{sc}$) also increases with the sensitization time initially and then becomes saturated. The open-circuit voltage ($V_{oc}$) and fill factor are stable with various sensitization times. These results suggest that $Zn_2SnO_4$ is stable against the acidic dye molecules. Otherwise, a fast increase in dye adsorption and a large decrease in the short-circuit current density should be observed due to the formation of aggregates as the case of ZnO.[10] The stability of $Zn_2SnO_4$ in an acidic dye solution is consistent with the previous report that $Zn_2SnO_4$ films can resist the acid etchant.[11]

The performance of $Zn_2SnO_4$ DSSCs with various film thicknesses was measured and compared with $TiO_2$-based DSSCs using


10.1021/ja070804f CCC: $37.00 

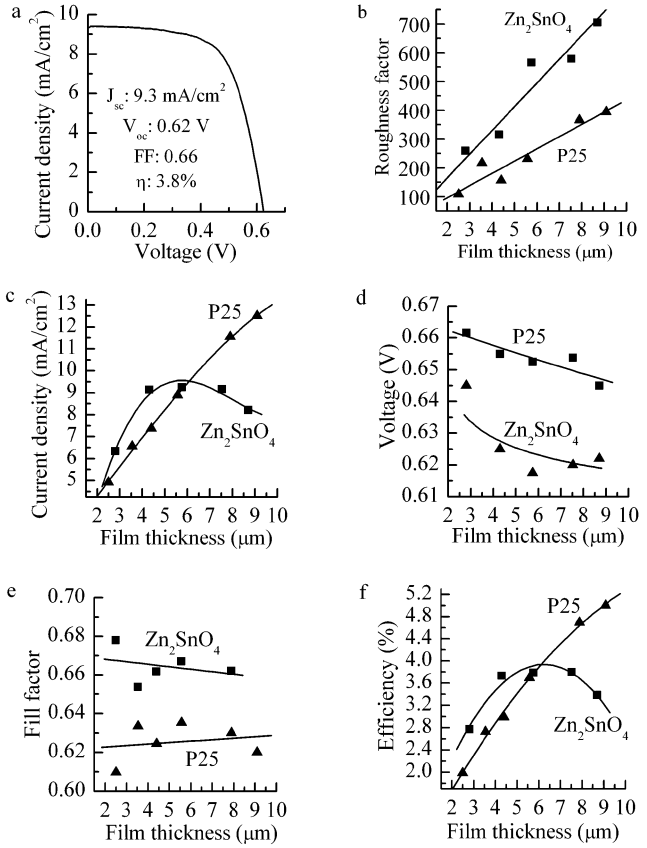


***Figure 2.*** (a) $I-V$ curve of a $Zn_2SnO_4$ cell with 5.6 $\mu$m film thickness. Dependence of cell performance on film thickness: (b) roughness factor; (c) short-circuit current density; (d) open-circuit voltage; (e) fill factor; and (f) overall light-to-electricity efficiency. All cells were under 1 sun AM 1.5 illumination.

P25 nanoparticles (Degussa; average size = 25 nm). All films made from $Zn_2SnO_4$ were transparent, while films made from P25 were translucent. For a fair comparison, all P25 films were prepared under similar conditions as $Zn_2SnO_4$ films without the treatment of $TiCl_4$ (see Supporting Information for the details of solar cell fabrication and measurement). The dye sensitization time was 1 day for all cells. Comparisons in dye adsorption, short-circuit current density, open-circuit voltage, fill factor, and overall light-to-electricity efficiency are shown in Figure 2.

Figure 2a shows a typical $I-V$ curve for the $Zn_2SnO_4$ cell. Figure 2b shows the dependence of roughness factor on film thickness. At 10 $\mu$m, the roughness factor for a $Zn_2SnO_4$ film is around 820, which is about twice the amount of dye adsorbed on a P25 film (roughness factor = 440). The high roughness factor for a $Zn_2SnO_4$ film shows that $Zn_2SnO_4$ can adsorb dye efficiently. The short-circuit current density for $Zn_2SnO_4$ cells increases initially from 2.8 to 4.3 $\mu$m, then becomes saturated from 4.3 to 7.5 $\mu$m, and finally drops down after 7.5 $\mu$m (Figure 2c). In comparison, the current density for P25 cells increases with thickness up to 9 $\mu$m. This shows that the electron diffusion length for $Zn_2SnO_4$ films is shorter than that for P25 films. For thin films ($\leq\sim$6 $\mu$m), the photocurrent density for a $Zn_2SnO_4$ cell is higher than that for a P25 cell of the same film thickness. However, considering the much higher dye loading on a $Zn_2SnO_4$ film, the electron injection and/or transport must be poorer in a $Zn_2SnO_4$ film than in a P25 film. The open-circuit voltage for a P25 cell is slightly higher than that of a $Zn_2SnO_4$ cell with the same thickness (Figure 2d), while the fill factor has the opposite relationship (Figure 2e). The overall light-to-electricity efficiency follows the same trend as the photocurrent density for both $Zn_2SnO_4$ and P25 cells (Figure 2f). For thin films ($\leq\sim$6 $\mu$m), the efficiency for a $Zn_2SnO_4$ cell is higher than that for a P25 cell. The highest energy conversion efficiency that we have achieved from a $Zn_2SnO_4$ cell is 3.8% with 5.6 $\mu$m film thickness.

The efficiency of 3.8% at 1 sun for a $Zn_2SnO_4$ cell is close to the highest efficiency reported for ZnO fabricated under similar conditions (4.1%[12]) and much higher than that reported for $SnO_2$ (1.2%[3]). $Zn_2SnO_4$ cells have also overcome the stability problem associated with ZnO against acidic dyes. In this sense, the ternary oxide ($Zn_2SnO_4$) is more attractive than its simple binary components (ZnO and $SnO_2$) as the electrode material for DSSC.

In summary, we have successfully synthesized $Zn_2SnO_4$ nanoparticles with desirable particle size from a hydrothermal process. We have demonstrated that the performance of $Zn_2SnO_4$ cells is comparable to that of $TiO_2$ cells in thin films. Because of its large band gap energy (3.6 eV), $Zn_2SnO_4$ cells could have better photostability against UV light than $TiO_2$ cells. Currently, the main limitation for $Zn_2SnO_4$ cells is the short electron diffusion length as indicated in the trend of $J_{sc}$ with increased film thickness. Detailed studies of electron transport dynamics in a $Zn_2SnO_4$ nanoparticle film and explorations of other multication oxides are under investigation.

**Acknowledgment.** We thank Dr. Patrick Woodward for providing the potentiostat. Acknowledgment is made to the donors of The American Chemical Society Petroleum Research Fund for partial support of this research.

**Supporting Information Available:** Procedure to fabricate and test $Zn_2SnO_4$ and P25 cells. This material is available free of charge via the Internet at http://pubs.acs.org.

## References

(1) (a) O'Regan, B.; Graetzel, M. *Nature* **1991**, *353* (24), 737. (b) Nazeeruddin, M. K.; Pechy, P.; Renouard, T.; Zakeeruddin, S. M.; Humphry-Baker, R.; Comte, P.; Liska, P.; Cevey, L.; Costa, E., Shklover, V.; Spiccia, L., Deacon, G. B.; Bignozzi, C. A.; Graetzel, M. *J. Am. Chem. Soc.* **2001**, *123* (8), 1613. (c) Gratzel, M. *J. Photochem. Photobiol., A: Chem.* **2004**, *164* (1−3), 3. (d) Chiba, Y.; Islam, A.; Watanabe, Y.; Komiya, R.; Koide, N.; Han, L. *Jpn. J. Appl. Phys. 2* **2006**, *45* (24−28), L638. (e) Mor, G. K.; Shankar, K.; Paulose, M.; Varghese, O. K.; Grimes, C. A. *Nano. Lett.* **2006**, *6* (2), 215.

(2) (a) Quintana, M.; Edvinsson, T.; Hagfeldt, A.; Boschloo, G. *J. Phys. Chem. C* **2007**, *111* (2), 1035. (b) Keis, K.; Magnusson, E.; Lindstrom, H.; Lindquist, S.-E.; Hagfeldt, A. *Sol. Energy Mater. Sol. Cells* **2002**, *73* (1), 51. (c) Law, M.; Greene, L. E.; Johnson, J. C.; Saykally, R.; Yang, P. *Nat. Mater.* **2005**, *4* (6), 455. (d) Martinson, A. B. F.; McGarrah, J. E.; Parpia, M. O. K.; Hupp, J. T. *Phys. Chem. Chem. Phys.* **2006**, *8* (40), 4655.

(3) Kay, A.; Graetzel, M. *Chem. Mater.* **2002**, *14* (7), 2930.

(4) (a) Guo, P.; Aegerter, M. A. *Thin Solid Films*, **1999**, *351* (1−2), 290. (b) Sayama, K.; Sugihara, H.; Arakawa, H. *Chem. Mater.* **1998**, *10* (12), 3825.

(5) Hara, K.; Horiguchi, T.; Kinoshita, T.; Sayama, K.; Sugihara, H.; Arakawa, H. *Sol. Energy Mater. Sol. Cells* **2000**, *64*, 115.

(6) Burnside, S.; Moser, J.-E.; Brooks, K.; Graetzel, M.; Cahen, D. *J. Phys. Chem. B* **1999**, *103* (43), 9328.

(7) Avelino, C.; Pedro, A.; Hermenegildo, G.; Jean-Yves, C.-C. *Nat. Mater.* **2004**, *3* (6), 394.

(8) Minami, T. *MRS Bull.* **2000**, *25* (8), 38.

(9) Coutts, T. J.; Young, D. L.; Li, X.; Mulligan, W. P.; Wu, X. *J. Vac. Sci. Technol. A* **2000**, *18* (6), 2646.

(10) (a) Keis, K.; Lindgren, J.; Lindquist, S.-E.; Hagfeldt, A. *Langmuir* **2000**, *16* (10), 4688. (b) Law, M.; Greene, L. E.; Radenovic, A.; Kuykendall, T.; Liphardt, J.; Yang, P. *J. Phys. Chem. B* **2006**, *110* (45), 22652.

(11) Morales-Acevedo, A. *Sol. Energy* **2006**, *80* (6), 675.

(12) Kakiuchi, K.; Hosono, E.; Fujihara, S. *J. Photochem. Photobiol. A: Chem.* **2006**, *179* (1−2), 81.

JA070804F